Available online at www.sciencedirect.com
SCIENCE DIRECT®
Biochemical and Biophysical Research Communications 338 (2005) 223–229
BBRC
www.elsevier.com/locate/ybbrc

Single-turnover kinetics of 2,3-dihydroxybiphenyl 1,2-dioxygenase reacting with 3-formylcatechol ☆

Tetsuo Ishida [a,*], Toshiya Senda [b], Hiroyuki Tanaka [a], Atsushi Yamamoto [a], Kihachiro Horiike [a]

[a] Department of Biochemistry and Molecular Biology, Shiga University of Medical Science, Seta, Ohtsu, Shiga 520-2192, Japan
[b] Biological Information Research Center, National Institute of Advanced Industrial Science and Technology, 2-41-6 Aomi Koto-ku, Tokyo 135-0064, Japan

Received 19 July 2005
Available online 7 September 2005

Abstract

2,3-Dihydroxybiphenyl 1,2-dioxygenase (EC 1.13.11.39) from *Pseudomonas* sp. strain KKS102 (BphC) catalyzes the proximal extradiol cleavage of the catechol ring of 2,3-dihydroxybiphenyl (DHB), a key step in the biodegradation of polychlorinated biphenyl. Because the active site Fe(II) ion of the extradiol dioxygenase is colorless, it has been difficult to monitor the reaction cycle kinetics. Here, we have found that BphC binds strongly the chromophoric substrate 3-formylcatechol (3FC) as a monoanion ($K_d = 0.8$ μM) and cleaves it two orders of magnitude slower compared to DHB under air-saturation conditions. By utilizing 3FC as a probe, the reaction cycle kinetics of BphC was monitored for the first time. The binding of 3FC occurred in a three-step process involving rapid deprotonation of 3FC. The bound monoanionic 3FC reacted slowly with O_2 in three steps, occurring in sequence, the ring opening step being the slowest one.

Keywords: Extradiol dioxygenase; Non-heme iron; Transient state kinetics; Catechol; Stopped-flow; Circular dichroism

Some soil bacteria degrade aromatic compounds including hazardous pollutants such as polychlorinated biphenyls and dioxins using O_2 [1–6]. In many catabolic pathways, the aromatic ring is first subjected to dihydroxylation, and then the resultant 1,2-dihydroxybenzene (catechol) derivative is cleaved between the C1 and C2 carbon atoms (intradiol cleavage) or between the C2 and C3 carbon atoms (extradiol cleavage). Extradiol catechol dioxygenases catalyze the latter mode of cleavage (Fig. 1) and most of them need one ferrous ion fixed to the active site in the 2-His-1-carboxylate facial triad motif [7]. To improve bacterial ability to degrade specific aromatic compounds, it is important to understand both the reaction mechanism of the extradiol cleavage and the molecular basis of substrate preferences [8–15].

2,3-Dihydroxybiphenyl 1,2-dioxygenase (EC 1.13.11.39) from *Pseudomonas* sp. strain KKS102 (BphC) belongs to the I.3.A subfamily [16] and prefers bicyclic substrates, and is involved in the biodegradation of polychlorinated biphenyl [17]. Because crystallographic investigation of BphC has been most advanced [18–22], mechanistic studies of BphC are important to understand the extradiol dioxygenase reaction. Recently, single-turnover kinetic investigation of homoprotocatechuate 2,3-dioxygenase has been carried out using 4-nitrocatechol as a chromophoric probe [23]. However, 4-nitrocatechol cannot be used as a probe for the reaction cycle of BphC because it is not a substrate of BphC but inactivates BphC in an O_2-dependent manner (manuscript in preparation). In addition, 4-nitrocatechol is an unusual substrate among most catecholic substrates (pK_{a1} 8–9.5) [24] in that it has a very low pK_{a1} value of 6.89 [23] and shows dianionic binding to homoprotocatechuate 2,3-dioxygenase [23], not the standard monoanionic

☆ *Abbreviations:* BphC, 2,3-dihydroxybiphenyl 1,2-dioxygenase from *Pseudomonas* sp. strain KKS102; DHB, 2,3-dihydroxybiphenyl; 3FC, 3-formylcatechol; *I*, ionic strength; Mpc, catechol 2,3-dioxygenase from *Pseudomonas putida* mt-2.

* Corresponding author. Fax: +81 77 548 2157.
E-mail address: teishida@belle.shiga-med.ac.jp (T. Ishida).

0006-291X/$ - see front matter © 2005 Elsevier Inc. All rights reserved.
doi:10.1016/j.bbrc.2005.08.218

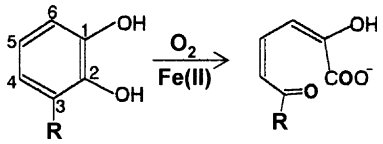

Fig. 1. Reaction catalyzed by BphC. R = phenyl, CHO, H.

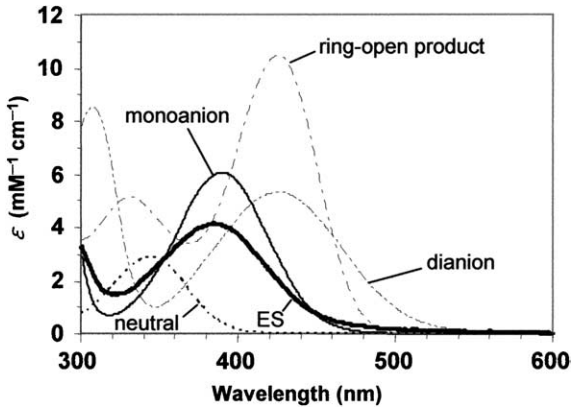

Fig. 2. UV/Vis spectra of 3FC species in solution and bound to BphC. Shown are spectra of neutral (···), monoanionic (––), and dianionic (-·-·-) 3FC in solution as well as BphC–3FC complex (thick solid line) and the cleavage product of 3FC (-·-), both at pH 7.5.

binding [25]. Therefore, another probe is needed to substantiate the results obtained using 4-nitrocatechol [23].

3-Formylcatechol (3FC) exhibits relatively strong absorbance in the wavelength region of 300–500 nm. Like 4-nitrocatechol, 3FC shows prominent spectral changes depending on the three ionization states (neutral form, monoanion, and dianion) (see Fig. 2). However, 3FC has the pK_{a1} value of 7.89 [24], showing one order of magnitude higher affinity to proton than 4-nitrocatechol. These features of 3FC are suitable for a probe to monitor the reaction cycle.

In this study, we have observed that BphC binds strongly 3FC as a monoanion and shows a small k_{cat} value under air-saturation conditions (0.8 s^{-1}). These properties of BphC for 3FC allowed us to perform single-turnover experiments using stopped-flow method. The reaction cycle of BphC was successfully monitored via spectral changes occurring in 3FC during the complete single-turnover.

Materials and methods

Reagents. Catechol was purchased from Tokyo Kasei Kogyo (Tokyo, Japan); 3FC and 2-hydroxypyridine *N*-oxide from Sigma–Aldrich Japan (Tokyo); 2,3-dihydroxybiphenyl (DHB) and ascorbate oxidase (EC 1.10.3.3) from Wako Pure Chemical Industries (Osaka, Japan); and L-ascorbic acid from Nacalai Tesque (Kyoto, Japan). Catechol and 3FC were recrystallized to remove minor contaminants. All other chemicals were of analytical grade. Catechol 2,3-dioxygenase from *Pseudomonas putida* mt-2 (Mpc) was prepared as described previously [26].

Overexpression of BphC in Escherichia coli and purification. BphC was overexpressed in *Escherichia coli* BL21(DE3)pLysS (Promega, Madison, WI, USA) transformed with pHNA2T7, an expression plasmid containing the structural gene encoding an enzyme described previously [19]. Purification of BphC was performed at about 4 °C in the presence of 0.2 mM of 2-hydroxypyridine *N*-oxide, a potent competitive inhibitor, and 10% acetone (vol/vol) according to the method used for the purification of Mpc with modifications [26]. The purified BphC samples were stored at about 4 °C in ammonium sulfate precipitates. During the storage for several months the amorphous precipitates changed into fine crystals.

Enzyme and iron quantification. The subunit concentration of purified BphC was determined using a molar absorption coefficient of the enzyme subunit at 280 nm of 3.82×10^4 M^{-1} cm^{-1}. Based on the maximal activity per iron atom (99 s^{-1}) observed during purification, we assumed that fully active BphC exhibits a specific activity of 185 U/mg under standard assay conditions (see below). The iron content of purified BphC was determined using the FeroZine method [27] after the complete digestion of samples by the method of Yonetani [28].

Handling of BphC. A concentrated BphC solution (300–500 μM) in 50 mM Hepes (pH 7.5, ionic strength (I) = 0.15 M adjusted with NaCl) was prepared just before use as follows. The ammonium sulfate precipitates of the enzyme were collected from about 300 μl of the BphC stock solution by centrifugation. The collected enzyme was dissolved in a minimum amount of 50 mM Hepes buffer containing 10 mM ascorbate (pH adjusted with 1 M NaOH to about 7.5) and incubated for 20–30 min on ice. After removal of a small amount of insoluble material by centrifugation, the supernatant was subjected to gel filtration on a Sephadex G-25 column (1.5 × 7 cm, Amersham Biosciences) equilibrated with 50 mM Hepes (pH 7.5, I = 0.15 M). The holo-enzyme content of the final Bphc preparation was always 0.5–0.6 as judged by the observed specific activity and anaerobic titration with 3FC.

An appropriately diluted BphC stock solution (2–6 μM for DHB and catechol, 100–200 μM for 3FC) for steady-state kinetic experiments was prepared in a sealed vial (3.0 ml) by the dilution of the concentrated BphC solution with an O_2-eliminating solution composed of L-ascorbate and ascorbate oxidase as described previously [24]. The activity of the resultant BphC solution (50–140 U/mg) was stable for several days, and no significant change in the enzyme activity was found during a series of kinetic experiments.

Steady-state kinetic measurements. Standard assay of BphC was performed in 3.0 ml of air-saturated 50 mM Hepes (pH 7.5, I = 0.15 M) with 90 μM DHB by following the formation of the reaction products using a UV-140 UV/Vis spectrophotometer at 25 °C (Shimadzu). One unit is defined as the amount of the enzyme that produces 1 μmol of 2-hydroxy-6-oxo-6-phenylhexa-2,4-dienoate per min under these standard assay conditions. The initial velocity as a function of catecholic substrate concentration was examined at 25 °C by following spectrophotometrically the formation of products as described above for the standard assay. The initial velocity as a function of O_2 concentration was measured by following the O_2 consumption using a 2.9-ml glass reaction vessel equipped with a Model 5331 Clark-type polarographic O_2 electrode (Yellow Springs Instruments, Yellow Springs, OH, USA). The O_2 concentration of the reaction mixture was controlled between 4 and 500 μM using a method described [29]. The enzymatic reaction was started by adding an aliquot of the diluted BphC stock solution (0.5–10 μl) taken out from the sealed vial with a microsyringe just before use. The signals from the spectrophotometer and the O_2 electrode were recorded with a Unicorder U-228 analogue recorder (Pantos, Kyoto, Japan), and they were calibrated by recording the rapid and complete cleavage of a known amount of catecholic substrates in the buffer using 0.5–2.0 μl of the concentrated Mpc stock solution. Initial velocity data were analyzed as a hyperbolic function of substrate concentration to determine K_m and V_{max}.

Partition ratio of BphC for DHB, 3FC, and catechol was determined by measuring the amount of products formed before the enzyme was completely inactivated (see Table 1).

Determination of the dissociation constant for 3FC. The dissociation constant (K_d) for 3FC was determined by titration into a BphC solution (49.3 μM) in 50 mM Hepes buffer (pH 7.5, I = 0.15 M) at 25 °C in an anaerobic cuvette with a silicon septum and a silicone plug as previously described [29]. The circular dichroism (CD) spectrum was measured over the range of 300–500 nm using a Jasco model J-600 CD spectrophotometer (Jasco, Tokyo, Japan). The addition of the ligand was repeated 10–15 times until the molar ratio of the ligand and the enzyme subunit increased

Table 1
Steady-state kinetic and thermodynamic parameters of BphC[a]

Parameter	3FC	DHB	Catechol
k_{cat} (s^{-1})	2.8 ± 0.8	115	32.5
k_{cat} (air-saturation) (s^{-1})	0.87 ± 0.02	99	28.5
K_{mA} (μM)	10.8 ± 1.6	0.46	58.9
K_{mO_2} (μM)	830 ± 250	39.6	34.7
K_d (μM)	0.81 ± 1.30	0.50	ND[b]
Partition ratio[c]	$(7.3 \pm 0.8) \times 10^3$	$(4.9 \pm 0.5) \times 10^4$	$(1.1 \pm 0.1) \times 10^4$

[a] The values were determined in 50 mM Hepes (pH 7.5, $I = 0.15$ M) at 25 °C, as described under Materials and methods.
[b] ND, not determined.
[c] Partition ratio represents the number of product molecules formed per molecule of active enzyme before the enzyme is inactivated.

to 1.5–2.0. Dependence of the difference between the CD spectrum of the mixture and that of the free enzyme (ΔCD) on the total 3FC concentration (L_t) was fitted to the following equation using the non-linear least-squares method

$$\Delta CD = 2\Delta CD_\infty L_t/(E_0 + K_d + L_t + \sqrt{(E_0 + K_d - L_t)^2 + 4K_d L_t}), \quad (1)$$

where ΔCD_∞ is the maximal CD difference and E_0 is the total concentration of the intact active site (or enzyme subunit in holo-form). The K_d for DHB was also determined by the same method as described above. The absorption spectrum of the bound 3FC was measured according to the same method, except that a UV/Vis spectrophotometer was used instead of the CD spectrophotometer.

Transient kinetic experiments. All experiments were conducted using an Applied Photophysics model SX.18MV stopped-flow device at 25 °C. To establish pseudo-first-order reaction conditions, 3FC (5.3–15.8 μM) was mixed with 70 μM BphC (4- to 13-fold excess), where all concentrations are after mixing. The reactions were monitored either at a selected wavelength or by using a diode array detector to record the spectra in the 300–600 nm range at each time point. The time courses for single-wavelength data ($A(t)$) can be fit to the following summed exponential functions using non-linear regression

$$A(t) = a_0 + a_1 e^{-t/\tau_1} + a_2 e^{-t/\tau_2} + a_3 e^{-t/\tau_3}, \quad (2)$$

where a_i and $1/\tau_i$ are the amplitude and reciprocal relaxation time of the ith exponential phase.

Results

Optical spectra of 3FC, BphC-3FC complex, and the cleavage reaction product

Fig. 2 shows the spectra of 3FC in its three ionization states and its anaerobic complex with BphC at pH 7.5. In solution at pH 7.5, 3FC exists in approximately 71% fully protonated states and 29% monoanion ($pK_{a1} = 7.89$, $pK_{a2} > 10$) [24]. The spectrum of the BphC–3FC complex reveals that the bound 3FC is in the monoanion form. When BphC was titrated with 3FC under anaerobic conditions (Fig. 3, inset), a positive broad CD band appeared at around 380 nm, confirming the monoanionic binding. The magnitude of the CD band increased in direct proportion to the 3FC concentration until the concentration increased to about half of that of the BphC subunit, allowing the determination of the K_d for 3FC to be 0.8 ± 1.3 μM and the holo-enzyme content to be 51% (Fig. 3). When BphC was titrated with DHB, a positive CD band was induced at around 310 nm (data not shown), and the K_d for DHB was obtained to be 0.50 μM.

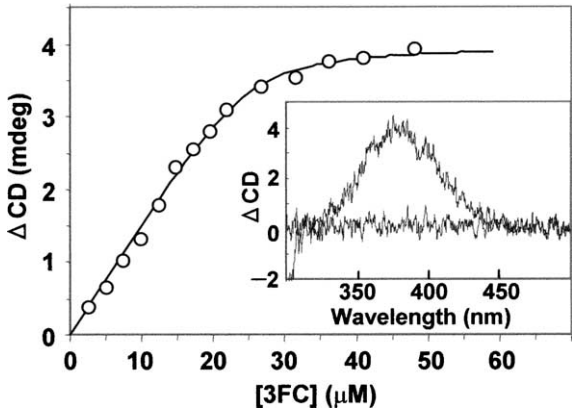

Fig. 3. Titration of BphC with 3FC. A BphC solution (3.0 ml, 49.3 μM) was titrated in 50 mM Hepes (pH 7.5) at 25 °C with 3FC in an anaerobic cell and the CD spectra between 300 and 500 nm were measured. The CD difference (ΔCD) at 381 nm between the BphC–3FC mixture and the free enzyme is plotted against the total concentration of 3FC. The solid line represents the best fit of Eq. (1) to the data. The inset shows the CD spectra observed for the titration mixture at 21.7 μM 3FC.

At pH 7.5, the 3FC ring cleavage product has an absorption maximum at 424 nm ($\varepsilon_{424} = 10{,}400\ M^{-1}\ cm^{-1}$) with a peak at 332 nm (Fig. 2). This spectrum was identical to that of the 3FC ring cleavage product by Mpc, indicating the proximal extradiol cleavage of 3FC.

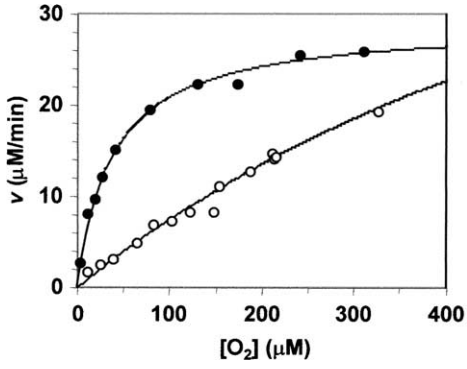

Fig. 4. The dependence of initial velocity on the O_2 concentration using 208 μM 3FC (○) and 81.8 μM DHB (●). The lines represent the best fits of Michaelis–Menten equation to the data. All experiments were performed using 50 mM Hepes (pH 7.5, $I = 0.15$ M) at 25 °C, and the enzyme concentration was 870 and 13 nM for 3FC and DHB, respectively.

The steady-state kinetic parameters and equilibrium binding data for 3FC, DHB, and catechol as substrates for BphC are summarized in Table 1. As shown in Fig. 4, BphC showed one order of magnitude higher K_m value for O_2 under a saturated concentration of 3FC compared with those of BphC for DHB and catechol.

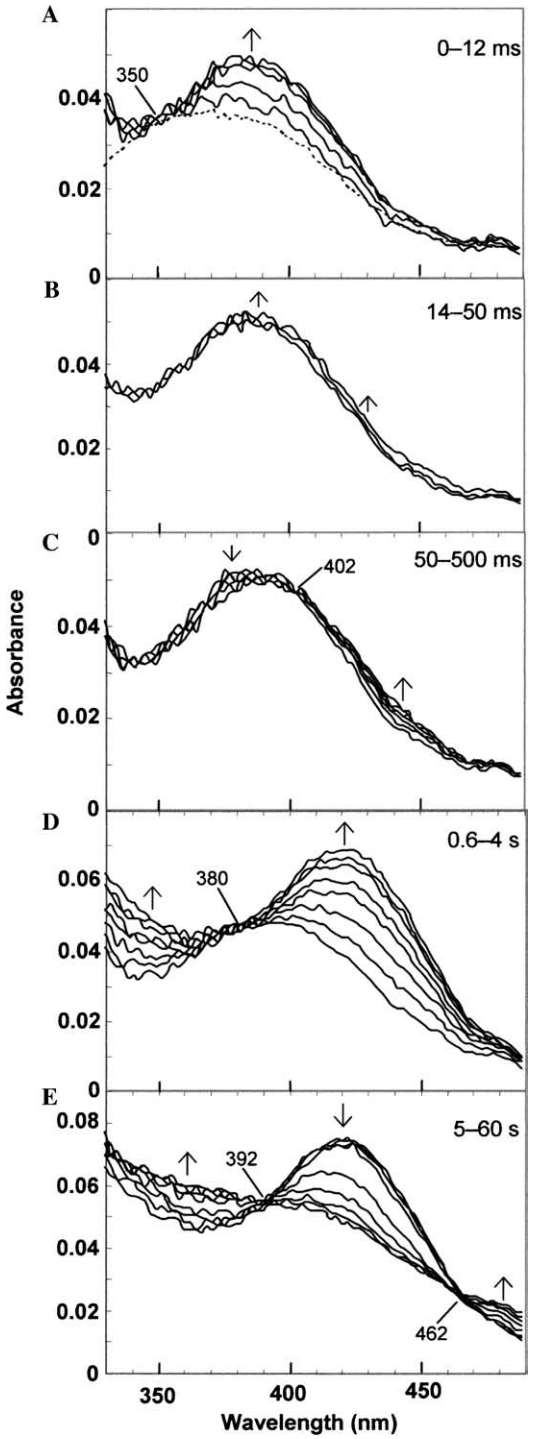

Fig. 5. Rapid scan diode array spectra of the single-turnover reaction of BphC reacting with 3FC. Five time intervals (A–E) of the time course are shown. Arrows indicate the direction of change in absorbance, and lines indicate isosbestic points. BphC (70 μM) was rapidly mixed with 10.5 μM 3FC in air-saturated 50 mM Hepes at pH 7.5, $I = 0.15$ M, and 25 °C, all the concentrations being after mixing. The dotted line in (A) is the spectrum of 10.5 μM 3FC. The absorbance background caused by the enzyme was removed by subtraction of a blank data set obtained with addition of different amounts of BphC.

Kinetics of the complete single-turnover cycle of BphC

To examine whether the bound monoanion observed thermodynamically under anaerobic conditions is actually an early intermediate prior to O_2 activation of the complete reaction, an excess amount of BphC (70 μM) was rapidly mixed with 5.28, 10.5, and 15.8 μM 3FC in air-saturated 50 mM Hepes (pH 7.5, $I = 0.15$ M), where all the concentrations are final ones after mixing. It is noted that these concentrations are in large excess over the K_d value of 0.8 μM.

Five time intervals of the diode array spectral data of the complete single-turnover reaction are shown in Fig. 5. The first segment of the reaction (0–12 ms, Fig. 5A) shows that the level of the monoanionic form of 3FC increases rapidly. In the following time interval of 14–50 ms, a slight further increase in the absorbance of the monoanionic species was observed (Fig. 5B). The third segment (50–500 ms, Fig. 5C) shows that the level of the monoanionic species of 3FC decreases with a concomitant increase in that of an intermediate, and an isosbestic point is seen near 402 nm: the absorbance around 440 nm increases and that around 370 nm decreases. The formation of the ring-open products is not detected at this stage of the reaction cycle. After a 0.6-s incubation, the absorbance at 420 and 330 nm started to increase with an isosbestic point at near 380 nm (Fig. 5D), indicating the formation of products from the intermediate. The last segment (5–60 s, Fig. 5E) shows the isomerization of the products (probably to a lactone species). Because the same spectral change was observed in steady-state kinetic conditions, this isomerization seems to be non-enzymatic one occurring in the released products.

To examine the transient kinetics, the time course of the BphC reaction was analyzed for three time intervals of 0–50 ms, 0.05–3.9 s, and 1–60 s by monitoring the absorbance at 386, 441, and 420 nm, respectively (Fig. 6). The time course of the BphC reaction within 50 ms after mixing was best fit by a summation of three exponential phases (Fig. 6A, Table 2). The obtained three reciprocal relaxation times did not significantly depend on the 3FC concentration (5.28–15.8 μM) used, supporting that pseudo-first-order reaction conditions are approximately established in the present experimental conditions by using an excess amount of BphC compared to 3FC. The half-life of the fastest step is 0.9 ms, nearly the dead time of the stopped-flow apparatus. This step shows negative amplitude. This possibly means that only neutral form of 3FC can go through the hydrophobic channel to the active site [20–22]. The largest spectral change observed within 50 ms after mixing (Fig. 5A) corresponds to the second phase, and it is suggested that 3FC is deprotonated to monoanion in this step. The third phase is one order of magnitude

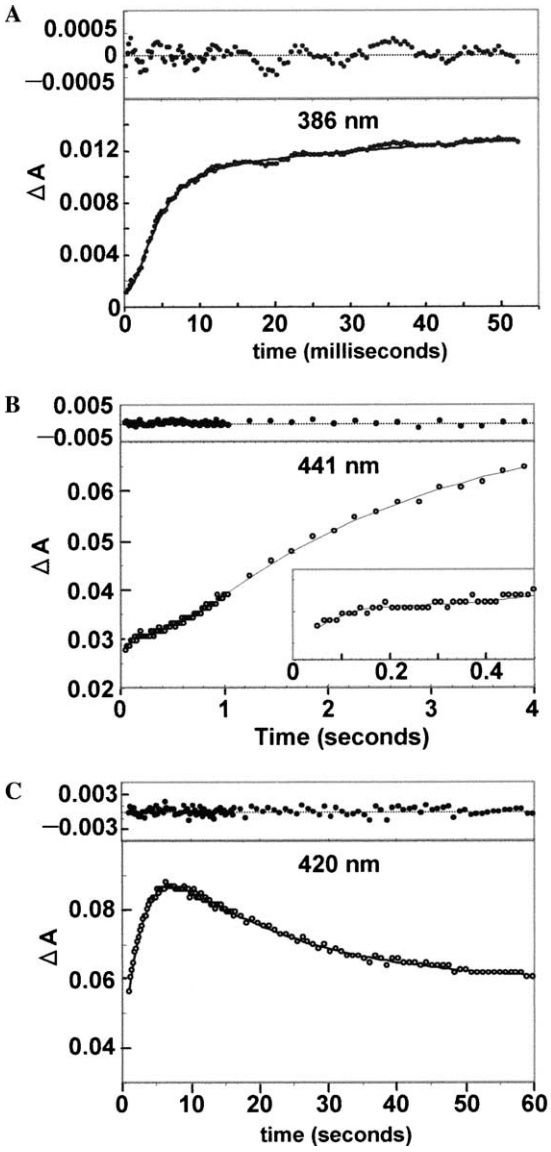

Fig. 6. Single-wavelength time course of the single-turnover reaction of BphC with 3FC. Progress curves monitored at 386 (A), 441 (B), and 420 nm (C) are shown for time intervals of 0–50 ms, 50 ms–3.9 s, and 1–60 s, respectively. The lines are three exponential fit (A and B) or two exponential fit (C), respectively. The residuals are shown above the each trace. The experimental conditions are the same as described in Fig. 5. The best-fit parameters are summarized in Table 2.

slower than the preceding two steps and small but significant increase in the magnitude of the monoanionic spectrum is observed (Figs. 5B and 6A), suggesting that the final monoanionic BphC–3FC complex is formed in this step. To verify that these relaxations represent steps leading to the formation of the BphC–3FC complex, we mixed argon-saturated solutions of BphC and 3FC. As shown in Fig. 7, the same transient change was observed for the initial part of the mixing under anaerobic conditions.

Fig. 6B shows the time course of the BphC reaction between 50 ms and 3.9 s after mixing as monitored at 441 nm. The observed time course was best fit by a summation of three exponential phases (Table 2). A new spectrum significantly different from those of the monoanionic 3FC species appeared between 50 and 500 ms (Fig. 5C), and this time-dependent spectral change is the first phase (Fig. 6B, inset), suggesting the formation of a ternary BphC–3FC–O_2 complex. This step is followed by a phase with a little slower reciprocal time and negative amplitude with the same magnitude. Due to this phase, the absorbance at 441 nm showed no change between 0.2 and 0.3 s. The third slowest phase becomes apparent after 0.5 s and corresponds to the product formation as judged by the spectral change (Fig. 5D). These results suggest that an intermediate is formed from the initial ternary complex before the start of the product formation.

The time course of the BphC reaction between 0.6 and 60 s after mixing as monitored at 420 nm was best fit by a summation of two exponential phases (Fig. 6C, Table 2). The first phase shows the product formation and is the same one as observed for the time-dependent change of absorbance at 441 nm as the third phase (Fig. 6B).

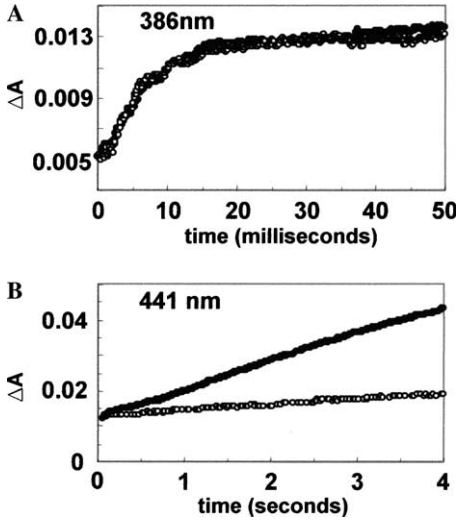

Fig. 7. Single-wavelength time course of the mixing of argon-saturated solutions of BphC and 3FC (○) in comparison with that under air-saturated conditions (●). Progress curves monitored at 386 (A) and 441 (B) are shown for time intervals of 0–50 ms and 50 ms–3.9 s, respectively. The experimental conditions are the same as those described in Fig. 5.

Table 2
Reciprocal relaxation times and phase amplitudes for BphC reactions[a]

Single-wavelength time course	Phase 1 (% total amplitude)	Phase 2 (% total amplitude)	Phase 3 (% total amplitude)
Absorbance at 386 nm (0–50 ms)	$772 \pm 64\ s^{-1}$ (−29.1)	$326 \pm 38\ s^{-1}$ (56.8)	$21.7 \pm 28.7\ s^{-1}$ (14.1)
Absorbance at 441 nm (0.05–3.9 s)	$9.69 \pm 0.98\ s^{-1}$ (21.3)	$4.75 \pm 0.75\ s^{-1}$ (−24.6)	$0.419 \pm 0.10\ s^{-1}$ (54.1)
Absorbance at 420 nm (0.6–60 s)	$0.378 \pm 0.081\ s^{-1}$ (59.6)	$0.0509 \pm 0.0159\ s^{-1}$ (−40.4)	

[a] Corresponding best-fit curves are drown in Fig. 6. The time course data at 420 nm (0.6–60 s) can be explained by two summed exponential functions.

The second phase is isomerization of the products (Figs. 5E and 6C).

Discussion

Examination of the transient kinetics of the extradiol dioxygenase reaction cycle is important to further the recent crystallographic studies [22,30,31] and theoretical studies [32,33] on the catalytic mechanism of non-heme iron extradiol dioxygenase. Recently, the transient kinetics of homoprotocatechuate 2,3-dioxygenase have been performed using the visible spectral change occurring on the strong chromophoric substrate 4-nitrocatechol [23]. However, 4-nitrocatechol is not a substrate but an inactivator of BphC. Although 4-nitrocatechol has been also used as a probe for Mpc, an important archetypal extradiol dioxygenases [23,34,35], spectral intermediates of the Mpc reaction cycle have not been detected until now mainly due to the efficient cleavage of 4-nitrocatechol by Mpc and the weak affinity of Mpc to 4-nitrocatechol. Therefore, another chromophoric substrate is needed to monitor the whole catalytic cycle of BphC and Mpc. The present work demonstrates that 3-formylcatechol can be used as such a probe for BphC.

3-Formylcatechol binds to BphC as strongly as DHB, indicating that the planar non-ionic substituent at the C3 position is important for the preference for bicyclic substrate. Unlike the transient kinetics of homoprotocatechuate 2,3-dioxygenase reacting with 4-nitrocatechol [23], the formation of the BphC–3FC complex is completed within 50 ms and there is about 200 ms lag time before the start of the formation of the ring-open products. Because the phenyl group of DHB is more bulky than the formyl group of 3FC, steric inhibition of the O_2 binding and activation is not likely. As we have demonstrated previously using the steady-state reaction of Mpc with various C3- and C4-substituted catechols [24], there is a strong negative correlation between the k_{cat}/K_{mO_2} and pK_{a1}. These findings reveal the importance of the electronic nature of the monoanionic binding state of catecholic substrate for the O_2 activation.

In the present study, multiple steps were observed for both the substrate binding process and the following reaction with O_2. To define the exact nature of these intermediates, detailed pre-steady-state kinetic analysis combined with crystallographic analysis is needed and is currently under way.

Acknowledgments

This work was supported by a Grant-in-Aid for Scientific Research on Priority Areas (B, NO. 753) (NO. 13125202) (to K.H., T. I., and H.T.) and a Grant-in-Aid for Scientific Research (C) (NO. 15590485) (to T.I. and H.T.) from the Ministry of Education, Culture, Sports, Science and Technology of Japan.

References

[1] G. Heiss, A. Stolz, A.E. Kuhm, C. Müller, J. Klein, J. Altenbuchner, H.J. Knackmuss, Characterization of a 2,3-dihydroxybiphenyl dioxygenase from the naphthalenesulfonate-degrading bacterium strain BN6, J. Bacteriol. 177 (1995) 5865–5871.

[2] A.E. Mars, T. Kasberg, S.R. Kaschabek, M.H. van Agteren, D.B. Janssen, W. Reineke, Microbial degradation of chloroaromatics: use of the *meta*-cleavage pathway for mineralization of chlorobenzene, J. Bacteriol. 179 (1997) 4530–4537.

[3] W.R. Abraham, B. Nogales, P.N. Golyshin, D.H. Pieper, K.N. Timmis, Polychlorinated biphenyl-degrading microbial communities in soils and sediments, Curr. Opin. Microbiol. 5 (2002) 246–253.

[4] J.J. Jeong, J.H. Kim, C.K. Kim, I. Hwang, K. Lee, 3- and 4-Alkylphenol degradation pathway in *Pseudomonas* sp. strain KL28: genetic organization of the lap gene cluster and substrate specificities of phenol hydroxylase and catechol 2,3-dioxygenase, Microbiology 149 (2003) 3265–3277.

[5] K. Maeda, H. Nojiri, M. Shintani, T. Yoshida, H. Habe, T. Omori, Complete nucleotide sequence of carbazole/dioxin-degrading plasmid pCAR1 in *Pseudomonas resinovorans* strain CA10 indicates its mosaicity and the presence of large catabolic transposon Tn4676, J. Mol. Biol. 326 (2003) 21–33.

[6] K. Inoue, J. Widada, S. Nakai, T. Endoh, M. Urata, Y. Ashikawa, M. Shintani, Y. Saiki, T. Yoshida, H. Habe, T. Omori, H. Nojiri, Divergent structures of carbazole degradative *car* operons isolated from gram-negative bacteria, Biosci. Biotechnol. Biochem. 68 (2004) 1467–1480.

[7] E.L. Hegg, L.J. Que, The 2-His-1-carboxylate facial triad. An emerging structural motif in mononuclear non-heme iron(II) enzymes, Eur. J. Biochem. 250 (1997) 625–629.

[8] J.L. Ramos, A. Wasserfallen, K. Rose, K.N. Timmis, Redesigning metabolic routes: manipulation of Tol plasmid pathway for catabolism of alkylbenzoates, Science 235 (1987) 593–596.

[9] K. Furukawa, Engineering dioxygenases for efficient degradation of environmental pollutants, Curr. Opin. Biotechnol. 11 (2000) 244–249.

[10] P.C. Cirino, F.H. Arnold, Protein engineering of oxygenases for biocatalysis, Curr. Opin. Chem. Biol. 6 (2002) 130–135.

[11] S. Dai, F.H. Vaillancourt, H. Maaroufi, N.M. Drouin, D.B. Neau, V. Snieckus, J.T. Bolin, L.D. Eltis, Identification and analysis of a bottleneck in PCB biodegradation, Nat. Struct. Biol. 9 (2002) 934–939.

[12] D.B. McKay, M. Prucha, W. Reineke, K.N. Timmis, D.H. Pieper, Substrate specificity and expression of three 2,3-dihydroxybiphenyl 1,2-dioxygenases from *Rhodococcus globerulus* strain P6, J. Bacteriol. 185 (2003) 2944–2951.

[13] F.H. Vaillancourt, M.A. Haro, N.M. Drouin, Z. Karim, H. Maaroufi, L.D. Eltis, Characterization of extradiol dioxygenases from a polychlorinated biphenyl-degrading strain that possess higher specificities for chlorinated metabolites, J. Bacteriol. 185 (2003) 1253–1260.

[14] K. Ohnishi, A. Okuta, J. Ju, T. Hamada, H. Misono, S. Harayama, Molecular breeding of 2,3-dihydroxybiphenyl 1,2-dioxygenase for enhanced resistance to 3-chlorocatechol, J. Biochem. 135 (2004) 305–317.

[15] A. Okuta, K. Ohnishi, S. Harayama, Construction of chimeric catechol 2,3-dioxygenase exhibiting improved activity against the suicide inhibitor 4-methylcatechol, Appl. Environ. Microbiol. 70 (2004) 1804–1810.

[16] L.D. Eltis, J.T. Bolin, Evolutional relationships among extradiol dioxygenases, J. Bacteriol. 178 (1996) 5930–5937.

[17] K. Kimbara, T. Hashimoto, M. Fukuda, T. Koana, M. Takagi, M. Oishi, K. Yano, Cloning and sequencing of two tandem genes involved in degradation of 2,3-dihydroxybiphenyl to benzoic acid in the polychlorinated biphenyl-degrading soil bacterium *Pseudomonas* sp. Strain KKS102, J. Bacteriol. 171 (1989) 2740–2747.

[18] K. Sugiyama, T. Senda, H. Narita, T. Yamamoto, K. Kimbara, M. Fukuda, K. Yano, Y. Mitsui, Three-dimensional structure of 2,3-dihydroxybiphenyl dioxygenase (BphC enzyme) from *Pseudomonas* sp. strain KKS102 having polychlorinated biphenyl (PCB)-degrading activity, Proc. Japan Acad. B 71 (1995) 33–35.
[19] K. Sugiyama, H. Narita, T. Yamamoto, T. Senda, K. Kimbara, N. Inokuchi, M. Iwama, M. Irie, M. Fukuda, K. Yano, Y. Mitsui, Crystallization and preliminary crystallographic analysis of a 2,3-dihydroxybiphenyl dioxygenase from *Pseudomonas* sp. strain KKS102 having polychlorinated biphenyl (PCB)-degrading activity, Proteins 22 (1995) 284–286.
[20] T. Senda, K. Sugiyama, H. Narita, T. Yamamoto, K. Kimbara, M. Fukuda, M. Sato, K. Yano, Y. Mitsui, Three-dimensional structures of free form and two substrate complexes of an extradiol ring-cleavage type dioxygenase, the BphC enzyme from *Pseudomonas* sp. strain KKS102, J. Mol. Biol. 255 (1996) 735–752.
[21] Y. Uragami, T. Senda, K. Sugimoto, N. Sato, V. Nagarajan, E. Masai, M. Fukuda, Y. Mitsui, Crystal structures of substrate free and complex forms of reactivated BphC, an extradiol type ring-cleavage dioxygenase, J. Inorg. Biochem. 83 (2001) 269–279.
[22] N. Sato, Y. Uragami, T. Nishizaki, Y. Takahashi, G. Sazaki, K. Sugimoto, T. Nonaka, E. Masai, M. Fukuda, T. Senda, Crystal structures of the reaction intermediate and its homologue of an extradiol-cleaving catecholic dioxygenase, J. Mol. Biol. 321 (2002) 621–636.
[23] S.L. Groce, M.A. Miller-Rosenberg, J.D. Lipscomb, Single-turnover kinetics of homoprotocatechuate 2,3-dioxygenase, Biochemistry 43 (2004) 15141–15153.
[24] T. Ishida, H. Tanaka, K. Horiike, Quantitative structure-activity relationship for the cleavage of C3/C4-substituted catechols by a prototypal extradiol catechol dioxygenase with broad substrate specificity, J. Biochem. 135 (2004) 721–730.
[25] F.H. Vaillancourt, C.J. Barbosa, T.G. Spiro, J.T. Bolin, M.W. Blades, R.F.B. Turner, L.D. Eltis, Definitive evidence for monoanionic binding of 2,3-dihydroxybiphenyl to 2,3-dihydroxybiphenyl 1,2-dioxygenase from UV resonance Raman spectroscopy, UV/Vis absorption spectroscopy, and crystallography, J. Am. Chem. Soc. 124 (2002) 2485–2496.
[26] T. Kobayashi, T. Ishida, K. Horiike, Y. Takahara, N. Numao, A. Nakazawa, T. Nakazawa, M. Nozaki, Overexpression of *Pseudomonas putida* catechol 2,3-dioxygenase with high specific activity by genetically engineered *Escherichia coli*, J. Biochem. 117 (1995) 614–622.
[27] M.D. Percival, Human 5-lipoxygenase contains an essential iron, J. Biol. Chem. 266 (1991) 10058–10061.
[28] T. Yonetani, Studies on cytochrome oxidase. III. Improved preparation and some properties, J. Biol. Chem. 236 (1961) 1680–1688.
[29] H. Nakajima, T. Ishida, H. Tanaka, K. Horiike, Accurate measurement of near-micromolar oxygen concentrations in aqueous solutions based on enzymatic extradiol cleavage of 4-chlorocatechol: applications to improved low-oxygen experimental systems and quantitative assessment of back diffusion of oxygen from the atmosphere, J. Biochem. 131 (2002) 523–531.
[30] A. Kita, S. Kita, I. Fujisawa, K. Inaka, T. Ishida, K. Horiike, M. Nozaki, K. Miki, An archetypical exradiol-cleaving catecholic dioxygenase: the crystal structure of catechol 2,3-dioxygenase (metapyrocatechase) from *Pseudomonas putida* mt-2, Structure 7 (1999) 25–34.
[31] M.W. Vetting, L.P. Wackett, L.J. Que, J.D. Lipscomb, D.H. Ohlendorf, Crystallographic comparison of manganese- and iron-dependent homoprotocatechuate 2,3-dioxygenases, J. Bacteriol. 186 (2004) 1945–1958.
[32] R.J. Deeth, T.D.H. Bugg, A density functional investigation of the extradiol cleavage mechanism in non-heme iron catechol dioxygenases, J. Biol. Inorg. Chem. 8 (2003) 409–418.
[33] P.E.M. Siegbahn, F. Haeffner, Mechanism for catechol ring-cleavage by non-heme iron extradiol dioxygenases, J. Am. Chem. Soc. 126 (2004) 8919–8932.
[34] Y. Kojima, N. Itada, O. Hayaishi, Metapyrocatechase: a new catechol-cleaving enzyme, J. Biol. Chem. 236 (1961) 2223–2228.
[35] C.A. Tyson, 4-Nitrocatechol as a colorimetric probe for non-heme iron dioxygenases, J. Biol. Chem. 250 (1975) 1765–1770.